



# **iJRASET**

International Journal For Research in  
Applied Science and Engineering Technology



---

# **INTERNATIONAL JOURNAL FOR RESEARCH**

IN APPLIED SCIENCE & ENGINEERING TECHNOLOGY

---

**Volume: 10    Issue: III    Month of publication: March 2022**

**DOI: <https://doi.org/10.22214/ijraset.2022.40599>**

**[www.ijraset.com](http://www.ijraset.com)**

**Call:  08813907089**

**E-mail ID: [ijraset@gmail.com](mailto:ijraset@gmail.com)**

# Design and Performance Analysis of Underwater Acoustic Sensor Networks

Ishrat Majeed<sup>1</sup>, Er. Jasdeep Singh<sup>2</sup>

<sup>1</sup>M. Tech Scholar, Computer Science Engineering, RIMT University Mandi Gobingarh, Punjab, India

<sup>2</sup>Assistant Professor, Department of Computer Science and Engineering, RIMT University Mandi Gobingarh, Punjab, India

**Abstract:** *The underwater acoustic sensor network (UASN) is essential for exploration missions and observation in demanding environments. The UASN'S connection route is acoustic waves, which limits its usefulness in comparison to ground sensor networks. This is the case because to its limited capacity, latency, and significant route loss. This article provides comprehensive research of the characteristics of UASN. We explore the functionality of underwater acoustic ad-hoc networks in the presence of disruptions. RF signals are used as a communication mechanism in wireless sensor networks, both terrestrial and aerial. However, in a sub-sea setting, such as deep-sea research, detecting and transmitting data needs a completely different method to underwater communication. The fact that the seas cover 70% of the earth's surface and contain massive amounts of unexplored riches cannot be ignored. The aquatic environment has largely escaped the effects of recent breakthroughs in wireless sensor networks (WSNS) and their broad application in latest studies and economic progress. Research on underwater acoustic sensor networks (UASNS) is developing at a snail's pace due to the difficulties in transferring most of the state-of-the-art of land and air based WSNS to its aquatic equivalent. The bulk of underwater activities rely on acoustic communication and specialized sensors that can endure the harsh environment of the oceans. The purpose of this study is to investigate how UASN works in different situations. End-to-end latency and energy consumption are examined in response to a variety of factors. We also investigate how well underwater acoustic ad-hoc networks perform when nodes are dispersed, and the network is large.*

**Keywords:** *Under water Acoustics, Sensor, Wireless Sensor Networks, Energy Consumptions.*

## I. INTRODUCTION

The study and monitoring of the underwater environment is becoming increasingly popular among academics and practitioners. The architecture of underwater acoustic sensor networks is influenced by the acoustic distribution mode, the limited travel time speed, the poor physical connection quality, and the associated deployment challenges (UASN).

UASN's research is split into two major areas. Its first approach is based on the wireless systems idea, with members of the network stationed at preset locations and interacting via a permanent infrastructure (base stations). Base stations can be mounted on surface buoys or on the ocean floor. Decentralized ad-hoc nets with multi-hop communication links are the focus of the second trend. This article introduces and investigates one-dimensional and double underwater networks.

The strength of UASN is subject to significant attenuation, which is dependent on the signal's distance and frequency, and the bandwidth is severely limited. Therefore, we assume multi-hop transmission in two-dimensional topology using nearest neighbor routing.

Such a paradigm, on the other hand, is inappropriate for UOWSNs since a node can only interact with other nodes within a fixed beam scanning angle around their transmission trajectory, i.e., optical wireless components are connected via unidirectional connectivity. In arbitrarily scaled sector graphs [13], a unidirectional communication link is generated between nodes  $n_i$  and  $n_j$  (i.e.,  $n_i \rightarrow n_j$ ) if and only if  $n_j$  is located inside  $n_i$ 's beam scanning angle. A directed reverse path (i.e.,  $n_j \rightarrow n_i$ ) is possible if  $n_i$  is inside  $n_j$ 's beamwidth or through another multi-hop path.

The degree of network connectivity and the performance of localization are inextricably linked, with one susceptible to the other's influence. The connectedness of a network is commonly used as a metric for a variety of performance criteria, such as survivability, robustness, and fault tolerance [12].

. A network is connected if at least one connecting path exists between any two nodes, and it is determined by the number of connections in the network. In this way, link dependability is inextricably linked to connectivity, which is largely impacted by focusing errors and optical module mismatch. The most typical sources of pointing and alignment issues include random movements of the sea surface [15], [16], depth dependent changes and deep currents [7], and oceanic turbulence [11]. Precision pointing, acquisition, and tracking (PAT) systems of optical transceivers are essential to sustain trustworthy single hop communications. The correct location of the UOWSN is crucial for three reasons.

Increased network connectedness, on the one hand, increases detection efficiency since having more paired length estimations reduces positioning errors intuitively. More exact location information, on the other hand, results in a more precise PAT mechanism, allowing for reliable single hop performance.

Changing the speed of light to sound also changes the mechanics of communication, causing propagation delay and temporal synchronization. Algae development on camera lenses [5], salt accumulation, sensor affectivity deterioration, and other frequent underwater problems make the sensors susceptible. Finally, because present underwater sensors have a larger footprint and need more power, and regular battery replenishment processes are very expensive, UASNs will have different energy needs than terrestrial WSNs. There has been very little research into underwater acoustic network installations, leaving the field wide open for future advancements.

As all fingerprint traffic flows to the gateway (GW), the available load inside a single neighborhood is inversely proportional to the concentration of hops that neighborhood is from the gateway, making traffic more susceptible to congestion as it approaches the gateway. Analyzing the performance of MAC protocols in a multi-hop topology is more complex due to other factors, in addition to the network's traffic characteristics. Half-duplex interaction, time- and space-varying signal propagation losses, which make modelling transmission error rates and link connections challenging, application limits such as reliable service, and sophisticated topology implementations are only a few of them. While having a full theory that addresses all of these problems are desirable.

UASN has been used underwater for ocean sampling, disaster prevention, and military purposes. Undersea pipelines, cables, and international borderlines may all be monitored using UASN. A string network (also known as a linear network) is required for this application, which is made up of a row of nodes connected by directed links.

## II. LITERATURE REVIEW

For both two- and three-dimensional designs, Pompili et al. [12] devised a computational deploying analysis. They demonstrated a two-dimensional triangular-grid deployment strategy that leverages the fewest number of sensors to offer outstanding sensing and communication coverage. In a triangular-grid deployment, sensors are positioned at the vertex of equilateral triangles. They calculated that overlapping sections of sensed data may be avoided when the length of an isosceles triangle  $d$  is 3 times the sensor range  $r$ . The number of sensors and the quantity of sensing coverage that can be accomplished are trade-offs. The authors studied the dynamics of a descending object and evaluated its trajectory under the effect of water current, which may be used to calculate the final position of a sinking object. The concept was conceived by Ibrahim and his colleagues.

Later, to increase network performance, they devised a heuristic-based multiple surface-level gateway deployment technique [14]. To identify the optimal gateway points from a mesh of millimeter possible locations, they used the greed search and the greed-interchange algorithm. The authors proposed a multi-sink design as well as rules for deciding the number and location of surface gateways in UASNs. However, sensor deployment is the double problem. Nazrul Alam and Haas set out to develop a node placement approach that would enable 100 percent sensing coverage of a 3D environment while minimizing the number of sensors needed [15]. The voluminous quotient is the ratio of a polyhedron's volume to the volume of its circumsphere, as defined by the authors of this research. For comprehensive 3D coverage, the smaller the volumetric quotient, the fewer nodes are required. The study looks at how many different space-filling polyhedrons, such as the cube, hexagonal prism, rhombic dodecahedron, and truncated octahedron, are deployed. Simulation studies show that truncated octahedral cells are the best approach, and that the higher the volumetric quotient, the fewer nodes are needed to meet coverage and connection standards.

Felemban et al. characterized the optimum node placement as a lumped parameter program with the objective of lowering leakage currents for a given monitored volume and number of sensor nodes [16]. Relay nodes are arranged adjacent to one other in 3D space to create tiled malformed octahedrons, as shown in [15]. The main difference is that they considered the characteristics of underwater acoustic routes. Full explanation that the number of nodes required to cover a particular volume path in order to obtain the optimal coverage ratio in a 3D region is influenced by the operation frequency.

## III. OBJECTIVES

- A. The purpose of this research is to investigate how UASN works in different situations.
- B. We will conduct a communication theoretic analysis of underwater acoustic ad-hoc networks in the presence of interference.
- C. The link between the number of network hops that can be sustained, end-to-end FEP, power, and bandwidth allotment will be investigated.
- D. We will evaluate and ensure that a considerable quantity of connection may be achieved by carefully setting the operating frequency, power, and bandwidth.



#### IV. METHODOLOGY

Novel systems must eliminate environmental barriers to achieve high data throughput. This chapter covers the broadcaster, recipient, and channel conditions in the design of a communication system.

##### A. Transceiver Structure Overview

A transceiver is a device that combines a transmitter and a receiver into one unit. A transceiver structure represents the communication system model employed in this study. Each component is responsible for ensuring that the system's weaknesses are minimised. The first limitation studied in this paper is ISI, which is a prominent source of high BER in UWA communication systems. As a result, one remedy to the ISI problem is to design a receiver that compensates for or reduces the ISI in the received signal using an equalisation process. This chapter is dedicated completely to the study of equalisers, and the supplied structure has been adjusted to allow for quick equalisation iterations, as equalisation is at the heart of this project. The implications of each component on the UWA communication system are outlined.

##### B. Transceiver Description

This section goes through each component of the transponder. Blocks from the transmitter and receiver are processed concurrently when it simplifies the interpretation, such as in Inter-leaver and De-inter-leaver.

- 1) *Information Source:* Any information source, assuming it is the output of a source encoder, provides an output that can be a random variable (RV), i.e., the data bits input on the Encoder block are categorised in statistical terms, which simplifies the transceiver design. Alternatively, if the relevant system output was known for sure (periodic), there would be no need to relay it [8]. In this situation, the Encoder block input sequence is thought to be random variables. To put it another way, all prior and future outputs are statistically unrelated to the current input. . The bits entering the Encoder are expected to be sampled from a Weibull distribution, which may or may not be true in practise. On the other hand, using an inter-leaver and redundant bits can help to ensure that.
- 2) *Encoder & Decoder:* Convolutional code is a type of forward error correction (FEC) or channel encoding technology that was first introduced by Elias in 1955 [9]. He showed how linear shift registers may be employed to create data stream redundancy. He also proved that the results were excellent when the codes were chosen at random. This discovery was noteworthy since it corresponded with Shannon's more scientific concepts [6], which established that for a given data transmission at a rate less than the channel capacity, there are procedurally generated codes that guaranteed arbitrarily high levels of dependability. A linear recurrent encoder with a 1/3 rate is shown in Figure 1. The rate is determined by the fact that the encoder creates three bits for every input bit. In practice, an encoder with Q inputs and Q outputs has rate /Q [11, 12]. In Figure 3.2, a binary data stream, Input, is fed into a shift-register circuit composed of a series of bits. At each consecutive input to the shift register, the values of the semiconductor chips are tapped off and added by a specified sequence, resulting in three outputted bits in this example. The output of the terminations can be multiplexed in a number of ways, resulting in a wide range of stream patterns.

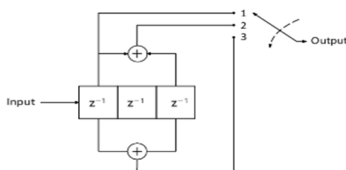


Figure 1: An 1/3-rate, K = 3 linear convolutional encoders.

Aside from the rate of the code and memory, another aspect that distinguishes a convolutional encoder from others is the restraint length. The constraint length K of a convolutional code is the maximum number of bits in a single output stream that may be influenced by any input bit, as well as the highest amount of shift register taps on the encoding circuit.

A circular encoder is like a finite-state machine. Therefore, the optimal decoder is a maximum likelihood sequence estimator (MLSE). The MLSE arrives at its conclusion after studying a succession of incoming signals over time. For the optimal decoding of a convolutional code, a search across the grid for the most likely sequence is necessary. Irrespective on whether the detector following the diplexer makes hard or soft judgements, the trellis search metric can be either a Hamming metric or a Euclidean metric [13].

We won't go into detail here, but the approach may reduce the number of sequences in the trellis search by deleting sequences when new deinterleave data is received. offer more details about the measurements and method

3) *Interleave & De-interleave*: Error-correcting codes may successfully repair errors as long as there aren't too many defects in a single codeword. Errors, on the other hand, tend to occur in surges, resulting in an existing store of damaged data [5]. Bursty error characteristics are present in multipath-enabled channels, such as the UWA channel. Signal fading induced by time-variant multipath propagation usually causes the signal to sink below the noise level, resulting in many errors. Error clusters are seldom repaired by codes that are optimised for statistically independent errors. An effective method for dealing with burst error channels is to interleave the coded data in such a way that the bursty channel is transformed into a channel with independent data. As a result, a code is used to handle distinct channel failures. Interleave is a technique for separating symbols from several code phrases during broadcast [5]. In Figure 2, the bits are input row by row and output column by column. An example of how to build an interleave is shown here. When the code words are reconstructed by the de-interleave, error bursts introduced by the channel are split up and scattered among many code words. The interleave/de-interleave combination produces a fundamentally random channel [8]. This attempt employs a random block inter-leaver, which picks a variations table at random using an initial seed value. By utilising the same initial seed value in the appropriate random de-inter-leaver block, the concatenated symbols can be restored to their original ordering. Figure 2 shows how data is inserted row by row and read column by column in a block inter-leaver.

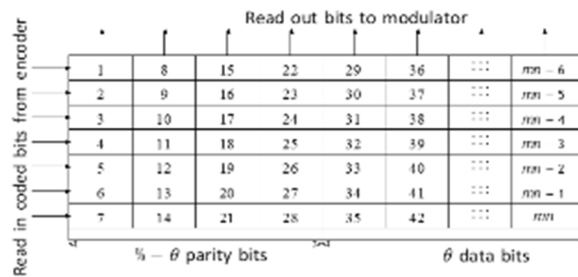


Figure 2: Example of block inter-leaver where data is inputted row-wise and read column-wise.

4) *Modulator & Demodulator*: A modulator converts a bit sequence into a waveform that may be sent via a network [4]. The modulator (demodulator analogously) may be split down into three sections, as shown in Figure 3. The Equalizer item is not displayed after the Square wave to Signals block in the preceding image for clarity, and the Detector section is made up of the Passband to Carrier frequency and Waveform to Signals blocks. . A technique for transferring a run of binary to a string of real or complex numbers, followed by a strategy for converting a sequence of numbers to a waveform, will be the necessary aspects of a modulating. A baseband waveform is converted to a bandpass waveform in the last part. The wideband harmonic is mapped back to baseband at the demodulator before both components of demodulation are completed. This is how the modulation procedure is carried out. The interleaved bits are turned into a waveform after being translated into constellation signals, such as M-PSK digital modulation [13]. Consider the mapped signal  $x[k] \in \mathbb{C} \subset \mathbb{C}$ , signal of a generic constellation  $\mathbb{C}$  and with sampling period  $T \in \mathbb{R}^+$ . This signal must first be transformed into a waveform before it can be broadcast. Up sampling is the initial step.

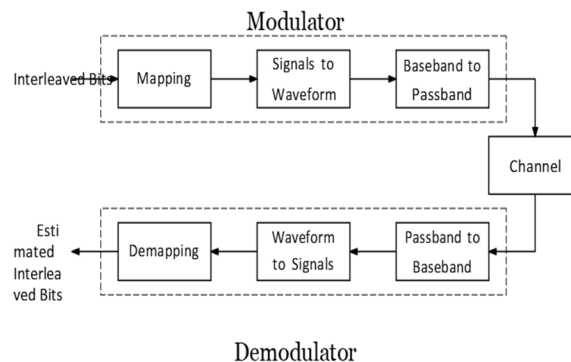


Figure 3: Illustration of modulator and demodulator structure

### C. Channel Estimation

The receiver was supposed to have entire knowledge of the CIR in the prior section; however, in practise, the receiver does not have comprehensive knowledge of the channel. As a result, the CIR must be calculated; the most frequent technique is to employ pilots during transmission. The pilots are a set of signals that both the transmitter and the receiver can recognise. In this study, the reception is considered as linear convolution, removing the AWGN's effect and reducing the estimation to a least-squares problem.

This design was made by

$$y = H\phi,$$

where  $\phi \in \mathbb{C}^{K \times 1}$  is the pilot vector. By the linear property of convolution, equation can be rewritten with  $\phi$  in a Toeplitz matrix form  $\Phi \in \mathbb{C}^{N \times K}$

$$y = \Phi h,$$

where  $h \in \mathbb{C}^{K \times 1}$  is the CIR. Equation (3.29) can be solved using least-squares, where it minimizes the squared error between  $y$  and  $\Phi h$ . The least-squares solution of equation is given by

$$\hat{h} = \Phi^H \Phi^{-1} \Phi y.$$

This estimated CIR  $\hat{h} \in \mathbb{C}^{K \times 1}$  is used on the simulations

## V. SYSTEM ARCHITECTURE

This subsection contains a detailed model of acoustic power usage and hop count. For the rest of this article, we'll utilise the number of nodes ( $N$ ) in the monitored zone. To transport packets to the base station, each node employs a multi-hop route.

The channels in the underwater acoustic model are characterised by a route loss that changes with signal frequency and distance. With increasing frequency and distance, the absorber loss increases, limiting the bandwidth that may be employed. The underwater acoustic model is briefly summarised in this section.

### A. Energy Acoustic Model

Underwater sound propagation is governed by the Sonar equations, as given in Ref. [11]. Active and passive solar systems are the two types of sonar systems. The proactive produces noises of its own and listens following echoes. On the other hand, the passive Sonar system listens for noises made by other sonars. One form of the equation, as given below, depicts passive sonar taken from Ref. [12].

$$SL(d, f) = A(d, f) + N(f) + SNR - DI \quad (1)$$

### B. Ambient Noise

The following four components can be used to simulate ambient noise in the ocean:

$$\begin{aligned} \text{Water turbulence (Nt), } & 10 \log(Nt(f)) & 17 & 30 \log(f). \text{ Surface-ship (Ns), } & 10 \log(Ns(f)) & 40 & 20(s - 0.5) \\ & 26 \log(f) & & & & & 60 \log(f - 0.03). \\ \text{Surface-ship (Ns), } & 10 \log(Ns(f)) & 40 & & 20(s - 0.5) & & 26 \log(f) - 60 \log(f - 0.03). \end{aligned}$$

- Breaking waves (Nw),  $10 \log(Nw(f)) = 50 + 7.5w^{1/2} + 20 \log(f) - 40 \log(f + 0.4)$ .

$$N(f) = Nt(f) + Ns(f) + Nth(f) + Nw(f) \quad (2)$$

where  $s$  is the shipping activity factor,  $0 \leq s \leq 1$ , and  $w$  is the wind speed in m/s. The overall power spectral density in dB re  $\mu$  per Hz of the ambient noise is given as the following:

### C. Attenuation

$A(d, f)$  is attenuation or path loss in acoustic channels. Inhibition is caused by two processes: energy dispersion and wave uptake. The main emphasis of energy spreading is the transmission range of acoustic waves<sup>12</sup>, whereas wave absorption is frequency dependent. Terahertz signals are more sensitive to absorber loss because of the conversion of acoustic energy to heat.

The path loss,  $A(d, f)$ , of acoustic signal with transmission range  $d$  in meters and frequency  $f$  in KHz is given in dB by<sup>3</sup>

$$A(d, f) = k \times \log(d) + \alpha(f)d \times 10^{-3} \quad (3)$$

where  $\alpha(f)$  is the absorption coefficient and  $k$  is the spreading factor caused by energy spreading. Commonly used values for  $k$  is 10, 15, and 20.3

### D. Absorption Coefficient

The absorption coefficient of sea water is expressed using a variety of models. Ainslie and McColm<sup>13</sup> offer a simple but accurate model.

**E. Propagation Delay**

Acoustic wave transmission in water is much slower than electromagnetic wave transport (i.e., five time slower). Atmospheric parameters such as temperature, salinity, and depth, on the other hand, impact propagation velocity. We expect stable salinity and temperatures in an underwater environment. The propagation velocity in meter/seconds is as follows:

Furthermore, the signal that was attenuated across the UWA channel is amplified on the receiver side. After that, a bandpass filter is used to reduce interference from beyond the required bandwidth, and the signal is sampled at the bandpass. . All the modules in Figure 4 between  $x\tilde{(t)}$  and  $y\tilde{(t)}$  are what is called channel in this work, comprised one block.



Figure 4 UWA communication system analog front-end.

$$c = 1.402385 \times 10^3 + 5.038813T - 5.799136 \times 10^{-2}T^2 + 3.287156 \times 10^{-4}T^3 - 31.398845 \times 10^{-6}T^4 + 2.787860 \times 10^{-9}T^5 \quad (5)$$

T is the temperature of the water in Celsius. This equation is true for temperatures ranging from 0 to 95 degrees Celsius. For a distance of d in metres, the propagation time is measured in seconds.

**F. Underwater Network Topology**

This section shows and describes three different network topologies. As indicated in the subsections below, the primary goal of these networks is to explore the performance of underwater networks in a range of conditions.[15]

- 1) *Two-Dimensional with Center-BS*: In this approach, several sensor nodes (N) are strewn over the deployed area at random (L L). The nearest neighbour strategy is used to connect the nodes in a tree. The base station (the tree root) is built on the seafloor and positioned in the centre of the deployed field, as illustrated in Figure 5. The data from each sensor node is relayed in a multi-hop manner to the base station.

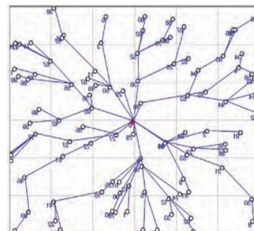


Figure 5: BS located at centre of the field

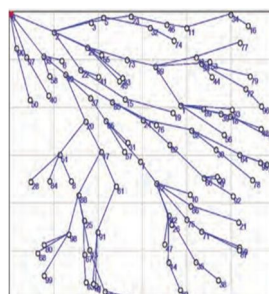


Figure 6: BS located at corner of the field.

- 2) *Two-Dimensional with Corner-BS*: With this architecture, a number of sensor nodes (N) are randomly scattered across a square field (L L). The tree is built using the nearest neighbour approach at the corner base station. The nodes seek the shortest multi-hop path to the base station. This topology, as shown in Figure 6, contains more in-between nodes (multi-hop) that relay data packets to the ultimate destination than the previous architecture.
- 3) *One-Dimensional Network (Linear)*: In this architecture, several sensor nodes (N) are uniformly placed in the shape of a line. The base station's position is the address is at the very end of the line. Each node only has two connections: the parent node at the top and the child node at the bottom. Each node generates a packet and transmits it, together with all packets received from the child and sub-child nodes to the parent node.

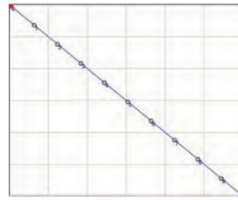


Figure 7: A portion of linear network.

### VI. RESULTS

The performance of the low-power wide-area network is demonstrated in this section. There has been a lot of simulations. Three different evaluation metrics are assessed, each of which is critical in an underwater sensor network. The first is the End-To-End delay, which is the amount of time it takes for data to travel from the source to the base station. Second, the amount of power necessary to transport data to the base station through multi-hop relay is referred to as energy usage. . Finally, we look at how frequency affects the performance of the submarine network. The position of the base station is taken into consideration. In addition, two types of networks are being studied: two-dimensional and one-dimensional networks. It is also indicated what assumptions were used in this article. These can help the reader understand the topic in all of its aspects. Some of the assumptions are as follows:

- Sensor nodes are dispersed at random in the distribution field. Furthermore, each node prepares a pre-formatted packet to be forwarded up the tree.
- Communication between nodes is symmetric, and the power consumption examined here is exclusively for packet transmission.

In terms of sensor nodes, Figures 9 and 10 depict the transmission rate of a two-dimensional and only one network, correspondingly. It's worth noticing that the transmission power in both networks increases as the number of sensor nodes (N) increases.

Table 1 Simulation Parameters

| Simulation parameters               | Values                  |
|-------------------------------------|-------------------------|
| Number of sensor nodes ( <i>N</i> ) | 100, 200, 300, 400, 500 |
| Packet length (bits)                | 1024                    |
| Data rate (bps)                     | 2000                    |
| Distance (m)                        | 100, 200, 300, 400, 500 |
| Salinity (S)                        | 35                      |
| Acidity (pH)                        | 8                       |
| Frequency (KHz)                     | 10, 20, 30, ..., 100    |
| Temperature (C)                     | 15                      |
| Spreading coefficient (K)           | 15                      |
| Signal-to-noise ratio (SNR)         | 88.5331                 |

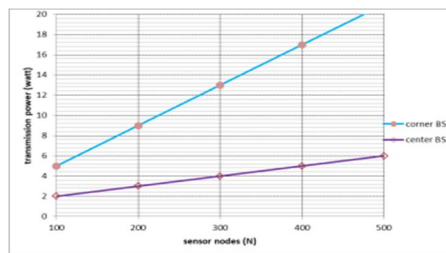


Figure 8: End delay versus sensor nodes.

The construction of a one-dimensional network causes a large boost in transmission power

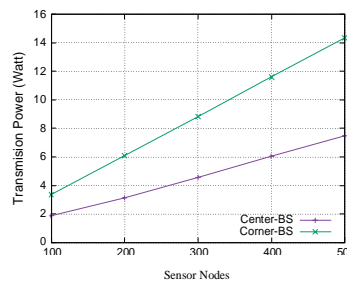


Figure 9: Transmission Power versus sensor nodes

Figure 9 shows, when we implement one dimensional network the transmission power gets immensely increased



Each leaf node starts by sending a packet to its parent node. The parent node then generates its own packet and transmits them both up the tree to the base station. As a result, adding nodes improves the power level, as shown in both pictures. The construction of a one-dimensional network causes a large boost in transmission power, as seen in Figure 8. This is owing to the structure of the linear network, which connects all sensors in a straight line. It's worth noting that, in all cases, the end-to-end latency increases as the distance between nodes increases. This is due to a longer propagation time for packet forwarding. When BS is in the middle, however, the delay is decreased to the shortest of all the options. The line network, on the other hand, illustrates the situation with the maximum latency.

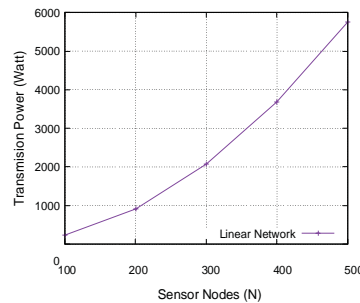


Figure 10: Sensor Nodes

Figure 10 shows the sensor nodes in one dimensional network when no external power is implemented

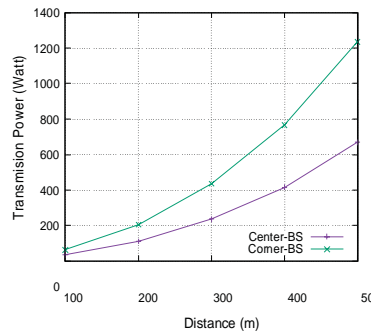


Figure 11: Transmission Power versus sensor nodes

Figure 11 shows the transmission power of a two-dimensional network wherein the power touches respective and relative hike

In terms of distance between sensor nodes, Figures 11 and 12 depict the transmission power of a two-dimensional and one-dimensional network, respectively. Clearly, energy consumed is related to distance, therefore even a little increase in distance results in an increase in transmission power. However, when BS is in the middle of the field, he gets the lowest score.

In terms of depth, Figures 13 and 14 indicate the network throughput of two-dimensional and one-dimensional data.

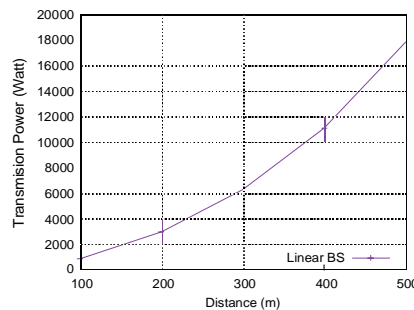


Fig 12: Linear Transmission versus distance

Figure 12: Linear transmission Power vs distance

This figure shows one dimensional Power and shows that as the distance increases energy consumed will also get increased.

The transmission power required to convey a packet from one sensor to another will, of course, grow as the depth force is increased. In contrast, as demonstrated in Figure 15, increasing the depth had no influence on the end-to-end latency.

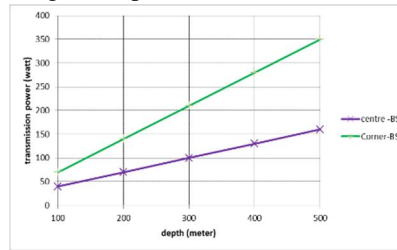


Figure 13: Transmission Power vs Depth

This figure shows the throughput of the two-dimensional network where power increases as the depth increases.

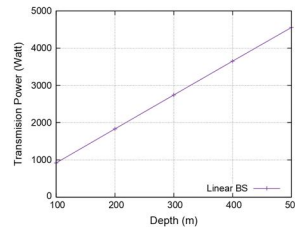


Figure 14: Linear Power vs Depth

As the depth increases the linear power similarly increases to the transmission power that shows that depth has a great influence on the transmission power.

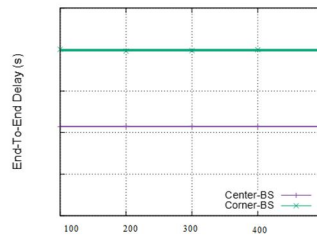


Figure 15: End Delay vs depth

Figure 15 shows that depth has no influence on end delay and is not altered by the alteration of the depth.

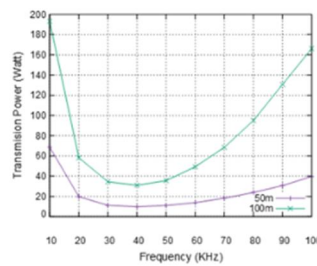


Figure 16: Transmission Power vs Frequency

Figure 16 shows the transmission power in terms of frequency. As can be observed, the 20 to 50 KHz range has the lowest transmission power. Past that point, frequency causes a large rise in transmission power.

## VII. CONCLUSION

The study and monitoring of the underwater environment are becoming increasingly popular among academics and practitioners. The bulk of underwater activities rely on acoustic communication and specialized sensors that can endure the harsh environment of the oceans. the purpose of this study is to investigate how UASN works in different situations.

We conducted a communication theoretic analysis of underwater acoustic ad-hoc networks in the presence of interference. The link between the number of network hops that can be sustained, end-to-end FEP, power, and bandwidth allotment was investigated. We observed that the network's whole connection zone can be constrained by coverage from below and hindrance from above. When the number of nodes in the network is low enough that the available power is insufficient to provide connectivity across a large area, the network is coverage limited. By selecting the suitable operating frequency and transmit power, the coverage-limited and interference-limited zones may be regulated. When the operating frequency is chosen to improve the SINR, the range of supported node densities (those for which complete connection is possible) is widest. If the operating frequency deviates from this value, or if the power is reduced below the minimum necessary to permit full connection, the range of supported densities narrows. In future, to locate underwater sensor networks, more research is needed. For underwater sensor networks, a GPS-like localization system has yet to be developed, and the location of a freely moving node is still a study topic. Aside from that, variable length packets in communication may be examined further. As a result, we plan to focus on variable packet size selection in the future to optimize acoustic channel use.

### REFERENCES

- [1] MACCURDY, E., Notebooks of Leonardo da Vinci. 1 ed. New York City, George Braziller, 1939.
- [2] NEWTON, I., Philosophiae Naturalis Principia Mathematica. 3 ed. London, J. Societatis Regiae ac Typis J. Streater, 1687.
- [3] MEDWIN H., CLAY S. C., Fundamentals of Acoustical Oceanography. 1 ed. Cambridge, Academic Press, 1998.
- [4] RAYLEIGH, J., The Theory of Sound. 2 ed. Cambridge, Cambridge University Press, 2011.
- [5] URICK, R. J., Principles of Underwater Sound. 3 ed. Newport Beach, Peninsula Pub, 1983.
- [6] FROST, G. L., "Inventing Schemes and Strategies: The Making and Selling of the Fessenden Oscillator", Technology and Culture, v. 42, n. 3, pp. 462–488, July 2001.
- [7] MANBACHI, A., COBBOLD, R. S. C., "Development and Application of Piezoelectric Materials for Ultrasound Generation and Detection", Ultrasound, v. 19, n. 4, pp. 187–196, November 2011.
- [8] CURIE, J., CURIE, P., "Development by Pressure of Polar Electricity in Hemihedral Crystals with Inclined Faces", Bulletin de la Societe de Minerologie, v. 3, n. 1, pp. 90, April 1880.
- [9] CURIE, J., CURIE, P., "Contractions and Expansions Produced by Voltages in Hemihedral Crystals with Inclined Faces", Comptes Rendus 93, v. 3, n. 1, pp. 1137–1140, February 1881.
- [10] ZHOU, S., WANG, Z., OFDM for Underwater Acoustic Communications. 1 ed. Hoboken, John Wiley & Sons, 2014.
- [11] LICHTHE, H., "On the Influence of Horizontal Temperature Layers in Seawater on the Range of Underwater Sound Signals", Physikalische Zeitschrift, v. 17, n. 1, pp. 385–389, September 1919.
- [12] LASKY, M., "Review of Undersea Acoustics to 1950", The Journal of the Acoustical Society of America, v. 61, n. 2, pp. 283–297, February 1977
- [13] KLEIN, E., "Underwater Sound and Naval Acoustical Research and Applications Before 1939.", The Journal of the Acoustical Society of America, v. 43, n. 5, pp. 931–947, July 1968.
- [14] XU, L., XU, T., Digital Underwater Acoustic Communications. 1 ed. Massachusetts, Academic Press, 2016
- [15] Noori, Roman. (2021). Network Security Attacks and Countermeasures on Layer 2 and Layer 3 Network Devices. International Journal for Research in Applied Science and Engineering Technology. 9. 1173-1185. 10.22214/ijraset.2021.33462..



10.22214/IJRASET



45.98



IMPACT FACTOR:  
7.129



IMPACT FACTOR:  
7.429



# INTERNATIONAL JOURNAL FOR RESEARCH

IN APPLIED SCIENCE & ENGINEERING TECHNOLOGY

Call : 08813907089  (24\*7 Support on Whatsapp)